J. D. Chung
Assistant Professor
e-mail: jdchung@sejong.ac.kr
Department of Mechanical Engineering,
Sejong University,
Seoul, 143-147,
Korea

A. J. H. McGaughey
Graduate Student
e-mail: amcgaugh@umich.edu

M. Kaviany
Professor
ASME Fellow
e-mail: kaviany@umich.edu

Department of Mechanical Engineering,
University of Michigan,
Ann Arbor, MI 48109-2125

Role of Phonon Dispersion in Lattice Thermal Conductivity Modeling

The role of phonon dispersion in the prediction of the thermal conductivity of germanium between temperatures of 2 K and 1000 K is investigated using the Holland approach. If no dispersion is assumed, a large, nonphysical discontinuity is found in the transverse phonon relaxation time over the entire temperature range. However, this effect is masked in the final prediction of the thermal conductivity by the use of fitting parameters. As the treatment of the dispersion is refined, the magnitude of the discontinuity is reduced. At the same time, discrepancies between the high temperature predictions and experimental data become apparent, indicating that the assumed heat transfer mechanisms (i.e., the relaxation time models) are not sufficient to account for the expected thermal transport. Molecular dynamics simulations may be the most suitable tool available for addressing this issue. [DOI: 10.1115/1.1723469]

Keywords: Conduction, Heat Transfer, Modeling, Properties

1 Introduction

The thermal conductivity of dielectric crystals (where phonons dominate the thermal transport) has been theoretically investigated since the works of Debye [1] and Peierls [2]. The exact or even numerical prediction of the thermal conductivity is a formidable task. This is due to the complexity of the Boltzmann transport equation (BTE), which is the basis for most solution techniques. Analytical thermal conductivity models have been developed based on the single mode relaxation time (SMRT) approximation in the BTE with different degrees of complexity [3,4]. In SMRT models, a single relaxation time is associated with each phonon mode, and describes how that mode would respond if excited while all others remain at equilibrium. The temperature and frequency dependencies of the relaxation times are assumed, and the predictions must be fit to the experimental data.

Callaway [3] developed an SMRT model that can successfully predict the low temperature thermal conductivity of germanium. This approach uses the Debye approximation, which assumes that there is no phonon dispersion and that the longitudinal and transverse polarizations behave identically. Holland [4] extended the work of Callaway by separating the contributions of longitudinal acoustic (LA) and transverse acoustic (TA) phonons, including some phonon dispersion, and using different forms of the relaxation times. Better high temperature agreement was found for germanium than with the Callaway model. The Holland model has been refined to include further detail on the phonon dispersion and relaxation times [5–7]. The added complexities lead to more fitted parameters. One could argue that the resulting better fits with the experimental data are due to this increase in the number of fitted parameters, and not to an improvement of the actual physical model.

This study examines the impact of refining the phonon dispersion model beyond the Debye approximation for germanium using an SMRT approach. Consideration is given to the distinction between the group and phase velocities, their frequency dependencies, and the rigorous treatment of impurity scattering. In the context of the improved dispersion model, some issues with the Holland relaxation time model are addressed.

Contributed by the Heat Transfer Division for publication in the JOURNAL OF HEAT TRANSFER. Manuscript received by the Heat Transfer Division June 13, 2003; revision received January 9, 2004. Associate Editor: G. Chen.

2 Thermal Conductivity Model

By solving the BTE and using the Fourier law of conduction, the thermal conductivity of germanium, assuming an isotropic crystal, and neglecting the contributions of optical phonons, has been predicted to be of the form [4]

$$k=\frac{1}{6\pi^2}\left[\int_0^{\omega_{mL}} c_v \frac{v_{g,L}}{v_{p,L}^2}\tau_L\omega_L^2 d\omega_L + 2\left(\int_0^{\omega_1} c_v \frac{v_{g,T}}{v_{p,T}^2}\tau_{T0}\omega_T^2 d\omega_T + \int_{\omega_1}^{\omega_{mT}} c_v \frac{v_{g,T}}{v_{p,T}^2}\tau_{TU}\omega_T^2 d\omega_T\right)\right]. \quad (1)$$

The first term corresponds to longitudinal (L) phonons, and the second and third terms to transverse (T) phonons (two degenerate branches). Here, c_v is the quantum-harmonic specific heat per normal mode and τ is a SMRT. The forms of τ are given in [4]. The upper limits of the first and third integrals are the angular frequencies of the phonon branches at the edge of the first Brillouin zone. For the transverse phonons, the frequency ω_1 is that at the center of the first Brillouin zone. The phonon group velocity, v_g, is defined as $\partial\omega/\partial\kappa$, where ω is the angular frequency and κ is the wave number. The phonon phase velocity, v_p, is defined as ω/κ.

3 Phonon Dispersion Models

Experimental results for the phonon dispersion of the acoustic modes of germanium in the [100] direction, at a temperature of 80 K, are shown in Figs. 1(a) and 1(b) [8]. The horizontal axis is a dimensionless wave number, which is obtained by normalizing the wave number against its value at the edge of the first Brillouin zone, i.e., $\kappa^*=\kappa/\kappa_m=\kappa/(2\pi/a)$. For germanium at a temperature of 80 K, the value of a is 5.651 Å [8]. To allow for the use of Eq. (1), which assumes isotropic dispersion, this direction is used in the subsequent analysis. The temperature dependence of the dispersion [9] is not considered. The experimental data at a temperature of 80 K are used for all calculations. To assess the importance of accurately modeling the dispersion, five different models are examined.

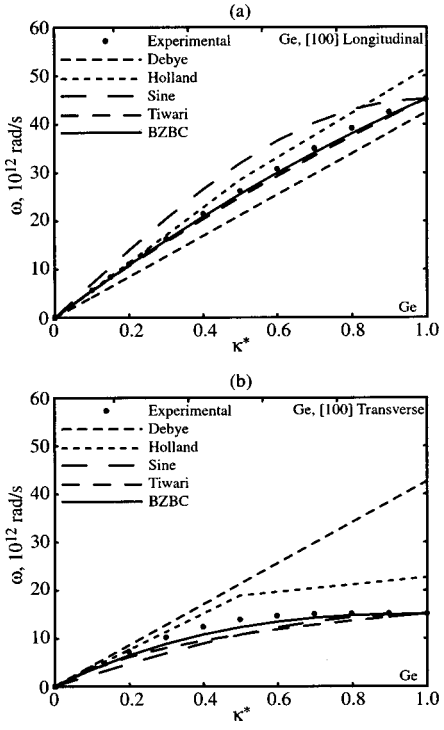

Fig. 1 Germanium phonon dispersion in the [100] direction. Experimental data [8] and five models used in this study for (*a*) LA phonons and (*b*) TA phonons.

3.1 Debye Model. From experimental data at low frequencies, the phonon frequency is proportional to its wave number such that

$$\omega = v_{0g}\kappa, \tag{2}$$

where the subscript 0 refers to the low frequency limit, i.e., $\kappa \to 0$, and v_{0g} is the low frequency limit of the phonon group velocity. The Debye dispersion model uses Eq. (2) for all frequencies, and does not distinguish between the LA and TA phonons. Note that in this case $v_p = v_g$, so that in Eq. (1), v_g/v_p^2 becomes $1/v_g$. The specification of v_{0g} is somewhat arbitrary. One possibility is [3]

$$\frac{1}{v_{0g}} = \frac{1}{3}\left(\frac{1}{v_{0g,L}} + \frac{2}{v_{0g,T}}\right), \tag{3}$$

where $v_{0g,L}$ and $v_{0g,T}$ are obtained from the experimental data. Using that of Nilsson and Nelin [8], we get 5142 m/s and 3391 m/s for $v_{0g,L}$ and $v_{0g,T}$, respectively, which give a v_{0g} value of 3825 m/s.

3.2 Holland Model. Holland [4] separated the contributions of LA and TA phonons, and included a partial effect of phonon dispersion by splitting each branch into two linear segments. The change in the slope (and thus the phonon velocities) is assumed to occur at a κ^* value of 0.5. As taken from the experimental data of Nilsson and Nelin [8], the phonon velocities $v_{0g,L}$, $v_{0g,T}$, $v_{0.5g,L}$, and $v_{0.5g,T}$ are 5142 m/s, 3391 m/s, 4152 m/s, and 678 m/s, where the subscript 0.5 refers to the segment between κ^* values of 0.5 and 1. Note that the change in slope implies that v_g is not equal to v_p in the second region. This effect was neglected by Holland, but is included in the current study.

3.3 Sine Function Model. In the sine function model, the phonon dispersion relation for each polarization is approximated by that of a linear monatomic chain as [10]

$$\omega_i = \omega_{mi}\sin\left(\frac{\pi\kappa_i^*}{2}\right), \tag{4}$$

where the label i can be L or T (this notation holds for the rest of the dispersion models). The critical drawback of this model is the nonrealistic behavior at low frequencies ($\kappa \to 0$) where the asymptotic velocities

$$v_{0g,i} = \left.\frac{\partial\omega_i}{\partial\kappa_i}\right|_{\kappa_i\to 0} = \frac{\pi\omega_{mi}}{2\kappa_{mi}} \tag{5}$$

are different from the experimental results. For $v_{0g,L}$ and $v_{0g,T}$, we obtain 6400 m/s and 2130 m/s, compared to the experimental values of 5142 m/s and 3391 m/s.

3.4 Tiwari Model. In the Tiwari model [5], the dispersion is assumed to be of the form

$$\kappa_L = \frac{\omega_L}{v_{0g,L}}(1+\alpha\omega_L) \quad \text{and} \quad \kappa_T = \frac{\omega_T}{v_{0g,T}}(1+\beta\omega_T^2), \tag{6}$$

where α and β are constants, given in [5]. Note that these equations satisfy the Brillouin zone boundary conditions

$$\kappa_i(\omega_i = 0) = 0 \quad \text{and} \quad \left.\frac{\partial\kappa_i}{\partial\omega_i}\right|_{\omega_i=0} = \frac{1}{v_{0g,i}}. \tag{7}$$

This model does not show the observed experimental behavior of

$$\left.\frac{\partial\omega_T}{\partial\kappa_T}\right|_{\kappa_T^*\to 1} = 0 \tag{8}$$

at the edge of the Brillouin zone, as seen in Fig. 1(*b*).

3.5 Present Study. We introduce a new model for the dispersion, referred to hereafter as the Brillouin zone boundary condition (BZBC) model. A quadratic wave number dependence for LA phonons and a cubic wave number dependence for TA phonons are used. This model is a modification of the Tiwari model, in that the boundary conditions given by Eqs. (7) and (8), and $\omega_i(\kappa_{mi}) = \omega_{mi}$, are applied. The resulting dispersion relations are

$$\begin{aligned}\omega_L &= v_{0g,L}\kappa_m\kappa^* + (\omega_{mL} - v_{0g,L}\kappa_m)\kappa^{*2}\\ \omega_T &= v_{0g,T}\kappa_m\kappa^* + (3\omega_{mT} - 2v_{0g,T}\kappa_m)\kappa^{*2}\\ &\quad + (v_{0g,T}\kappa_m - 2\omega_{mT})\kappa^{*3}.\end{aligned} \tag{9}$$

3.6 Comparison of Dispersion Models. A comparison of the five dispersion models, along with the experimental data for germanium [8], is shown in Figs. 1(*a*) and 1(*b*). For the both the longitudinal and transverse polarizations, both the Tiwari and BZBC models match the experimental data reasonably well over most of the first Brillouin zone. The agreement is not as good for the transverse polarization above κ^* values of 0.7 due to the plateau behavior, which is difficult to fit with a low order polynomial. The other dispersion curves are unsatisfactory. Of the Tiwari and BZBC models, the BZBC curve gives the best agreement with the experimental data. We note than none of these dispersion relations will be consistent with the experimental phonon density of states due to the isotropic assumption. Additionally, the integral of the volumetric density of states will not go to the expected value of $3n$, where n is the volumetric density of unit cells. In order for this to occur, one would need to set the dispersion with this result in mind. For these calculations, we are more concerned with matching the experimental dispersion data.

While the Tiwari and BZBC dispersion curves show some similarities, significant differences become apparent when the quantity they affect in the thermal conductivity expression, v_g/v_p^2, is considered. This is shown in Figs. 2(*a*) and 2(*b*). The deviation is most significant for the TA phonons near the edge of Brillouin zone, and will result in an over prediction of the high frequency contribution to the thermal conductivity by the Tiwari model. This

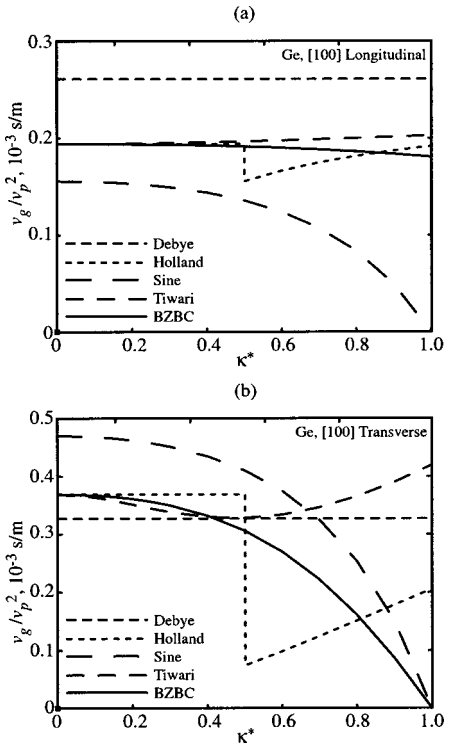

Fig. 2 v_g/v_p^2 for the five dispersion models plotted as a function of normalized wave number for (*a*) LA phonons and (*b*) TA phonons.

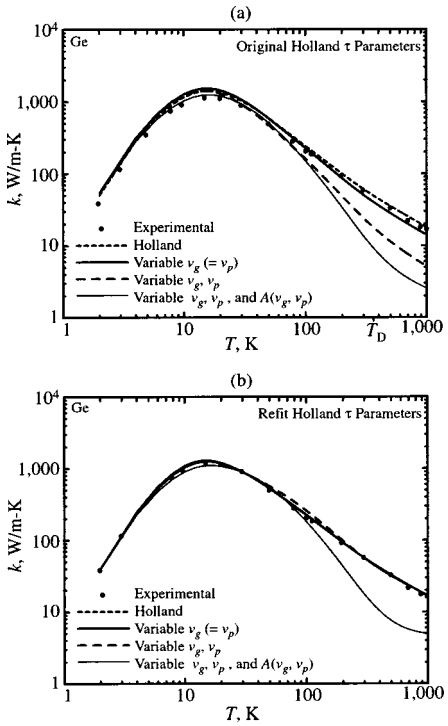

Fig. 3 Effect of refining the treatment of the dispersion on the prediction of the thermal conductivity of germanium. (*a*) Based on the original Holland fitting parameters, and (*b*) predictions refit to the experimental data.

deviation is because the appropriate boundary condition at the edge of the Brillouin zone (Eq. (8)) has not been enforced in the Tiwari model.

3.7 Impurity Scattering. The value of the thermal conductivity is sensitive to impurities, which include the isotopic content of an otherwise pure crystal [11]. The impurity relaxation time, τ_I, is given by [12,13]

$$\frac{1}{\tau_I} = \frac{V_0 \Sigma_i f_i [1-(M_i/M)]^2}{4\pi v_g v_p^2} \omega^4, \tag{10}$$

where V_0 is the average volume of a unit cell, f_i is the fractional concentration of species i, M is the average atomic mass, and M_i is the atomic mass of species i. At low frequency, where $v_g \sim v_p \sim v_{0g}$, the relaxation time displays an ω^{-4}-dependence (i.e., Rayleigh scattering). Due to phonon dispersion, such an assumption will not be valid at higher frequencies, and will lead to an overestimation of the thermal conductivity.

4 Thermal Conductivity Prediction

4.1 Role of Dispersion. The accuracy of the thermal conductivity model described in section 2 depends on the nature of the phonon dispersion and relaxation time models. To isolate the effects of dispersion, the relaxation time model used in the subsequent calculations is fixed to that of Holland [4].

In Figs. 3(*a*) and 3(*b*), the effect of including the difference between the phonon group and phase velocities on the prediction of the thermal conductivity of germanium is shown. The experimental data are taken from Holland [4]. The predicted values in Fig. 3 correspond to (i) the Holland model, that is, no distinction between v_g and v_p and a linear two region treatment, (ii) no distinction between v_g and v_p, but using the frequency dependence of the group velocity, (iii) different and frequency dependent v_g and v_p, and (iv) same as (iii), plus rigorous treatment of the impurity scattering by distinguishing between v_g and v_p. In (ii)–(iv), the velocities are calculated with the BZBC dispersion model. In (i)–(iii) the impurity scattering is calculated with $v_g = v_p = v_{0g}$ for each polarization.

In Fig. 3(*a*), the relaxation time model and fitting parameters originally obtained by Holland are used. In Fig. 3(*b*), the curves have been refit to the experimental data. From Fig. 3(*a*), it is evident that the fitting parameters are not universal, and strongly dependent on the dispersion model. Thus, to use the values obtained by Holland, one must also use that dispersion model. However, as shown in Fig. 3(*b*), by refitting the relaxation time parameters, excellent agreement with the experimental data can be obtained in all cases, except when the impurity scattering is rigourously modeled. In this case, the predicted thermal conductivity becomes lower than the experimental data, especially at high temperatures. Under the Holland dispersion, the plateau in the TA dispersion curve is not properly addressed, and the TA phonons make a significant contribution to the thermal conductivity at high temperatures. Here, with the proper modeling of the TA phonons, this contribution is reduced and as such, the role of TA phonons should be reassessed. The effect is not seen at low temperatures, where it is the lower frequency phonons that dominate the thermal transport.

4.2 Role of Relaxation Time Model. The use of a rigorous model for the phonon dispersion has led to an apparent failure of the Holland SMRT approach at high temperatures. The explanation for this must lie in the forms of the relaxation times used. While exact expressions for the relaxation times can be developed [14], their evaluation is extremely difficult due to the required knowledge of the phonon dispersion and three-phonon interactions. Approximate expressions are generally based on low frequency asymptotes [3,4], and yet are often applied over the entire temperature and frequency ranges.

Even with the observed disagreement, the importance of modeling the dispersion can still be shown. The Holland relaxation times are plotted in Fig. 4(*a*) at a temperatures of 80 K for the four

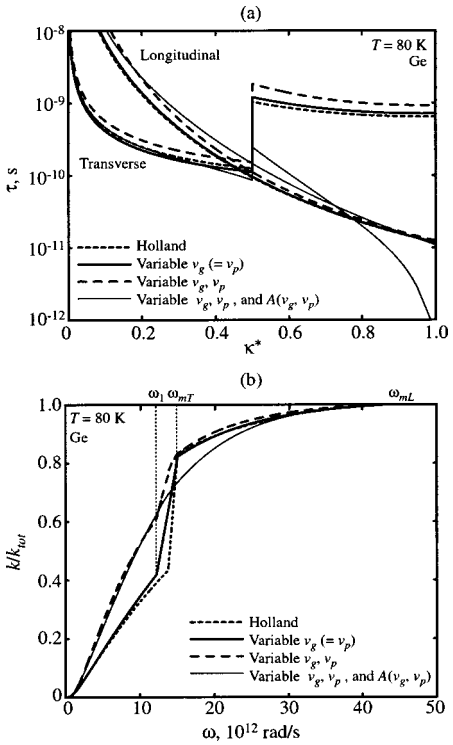

Fig. 4 (*a*) Three phonon relaxation times for refit data from Fig. 3(*b*) at $T=80$ K. (*b*) Cumulative frequency dependence of the thermal conductivity for refit data from Fig. 3(*b*) at $T=80$ K. The thermal conductivity is plotted as a percentage of the total value for each case. The curves show three distinct regions. The transition between the first and second regions takes place at ω_1, where the form of the TA relaxation time changes. The transition between the second and third regions occurs at ω_{mT}, after which there is no contribution from TA phonons [see Eq. (1)].

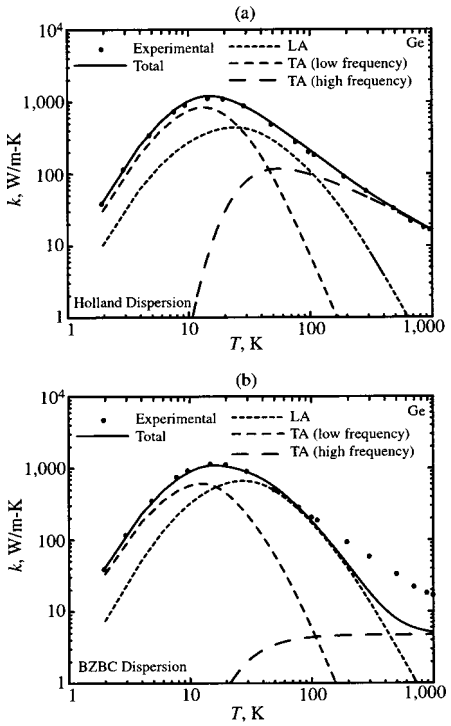

Fig. 5 Contributions of LA and TA phonon branches to the thermal conductivity based on (*a*) Holland dispersion model, and (*b*) BZBC dispersion model.

cases shown in Fig. 3(*b*). The most striking feature of these results is the large discontinuity in the TA relaxation time when κ^* is equal to 0.5, where the functional form is assumed to change (see Eq. (1)). As the temperature increases, the size of the discontinuity increases. For example, at a temperature of 900 K, the discontinuity covers four orders of magnitude. The size of the discontinuity decreases as the treatment of the dispersion is refined. This suggests that the observed behavior is more realistic. Such discontinuities are also found in other relaxation time models [5,6]. In theory, one would expect the relaxation time curves to be continuous, and this has been found in molecular dynamics simulations of the Lennard-Jones face-centered cubic crystal [15].

The effect of the fitting parameters in the relaxation time model can also be demonstrated by plotting the cumulative frequency dependence of the thermal conductivity. This is shown for the same four cases as Fig. 4(*a*) in Fig. 4(*b*). Note that the thermal conductivity is normalized against the total value for each case. As the treatment of the dispersion is refined, the thermal conductivity curves become smoother.

4.3 Transverse and Longitudinal Phonon Contributions The relative contributions of LA and TA phonons to the total heat flow at high temperatures have not been fully resolved. As shown in Fig. 5(*a*), the Holland model predicts that the TA phonons are the dominant heat carriers at high temperatures, even though they have lower group velocities than LA phonons. This result was supported by Hamilton and Parrott [16] using calculations based on a variational method, which does not involve the SMRT approximation. Mazumder and Majumdar [17] ascertained that above 100 K, TA phonons are the primary carriers of energy in silicon (which has the same crystal structure as germanium) using Monte Carlo simulations. However, their calculations were based on the original Holland relaxation times for silicon, which may have contributed to this conclusion. Asen-Palmer et al. [7] have concluded that while the heat flow in germanium above the maximum is primarily due to TA phonons, the LA Umklapp processes cannot be ignored (as they are in the Holland formulation). Ju and Goodson [18] have suggested that LA phonons are the dominant heat carriers in silicon near room temperature. Sood and Roy [6] ascertained that LA phonons dominate heat transport in germanium at high temperatures.

In Fig. 5(*b*), the relative contributions of LA and TA phonons to the thermal conductivity predicted by the BZBC dispersion model (with refit relaxation time parameters) are shown. Compared to the results of Fig. 5(*a*), the role of TA phonons is quite different when the dispersion and impurity scattering are rigorously modeled. We find a thermal conductivity of 5.2 W/m-K at a temperature of 1,000 K, while the experimental value is 17 W/m-K. The high frequency TA phonons cannot contribute much to the thermal conductivity of germanium because of their low group velocity, which appears directly in the thermal conductivity expression, and also results in a high impurity scattering rate. We note that the expected electronic contribution to the thermal conductivity of germanium at a temperature of 1,000 K is 4 W/m-K [19], which is not sufficient to explain the predicted discrepancy.

5 Summary

While the Holland approach to phonon thermal conductivity modeling has been used for more than forty years, some of its physical features are masked by the necessary use of fitting parameters. Previous work has thus only shown the qualitative validity of the SMRT approach. Using molecular dynamics simulations, it has recently been shown that the SMRT approach is also quantitatively valid for Lennard-Jones crystals, through careful

calculation of the relaxation times, and inclusion of the effects of temperature on the phonon dispersion [15]. This suggests that the analytical approach described here is valid, but must include accurate, physical modeling of the phonon dispersion and relaxation times. In this study, we have addressed the issue of the phonon dispersion (albeit isotropic, and neglecting any temperature effects) for germanium, using an existing relaxation time model.

Compared to the standard Debye approach, the rigorous treatment of the phonon dispersion has two effects, namely, (i) the use of v_g/v_p^2 in Eq. (1) instead of $1/v_g$, and (ii) enhancement of the impurity scattering rate, τ_I by using $1/v_p^2 v_g$ instead of $1/v_g^3$ in Eq. (10). As shown in Fig. 3(*b*), the effects of refining the dispersion are masked by the fitting parameters required in this approach for all cases except when the impurity scattering is properly modeled. Through examination of the relaxation times and the cumulative frequency dependence of the thermal conductivity, as shown in Figs. 4(*a*) and 4(*b*), the underlying behavior is found to be nonphysical, but improves as the treatment of the dispersion is refined.

To make up the difference in the experimental and predicted thermal conductivities, we suggest inclusion of two heat transfer mechanisms, namely, an optical phonon component [20] and/or an increased contribution of high frequency LA phonons. The role of LA phonons has been investigated to some extent in the past, but not in the context of an accurate dispersion model. We note that one must be very careful when using and/or formulating relaxation time models, as they should be continuous, and not contain abrupt order of magnitude changes. Molecular dynamics simulations appear to be the most promising source of such relations [15].

Acknowledgment

This work was supported by Korea Research Foundation grant KRF-2002-005-D20001 (JDC), the U.S. Department of Energy, Office of Basic Energy Sciences grant DE-FG02-00ER45851, and the Natural Sciences and Engineering Research Council of Canada (AJHM).

References

[1] Debye, P., 1914, *Vortrage uber die kinetische Theorie der Materie und der Elektrizitat*, Teubner, Berlin.
[2] Peierls, R., 1997, ''On the Kinetic Theory of Thermal Conduction,'' *Selected Scientific Papers of Sir Rudolf Peierls With Commentary*, Dalitz, R. H. and Peierls, R., eds., World Scientific, Singapore, pp. 15–48.
[3] Callaway, J., 1959, ''Model for Lattice Thermal Conductivity at Low Temperatures,'' Phys. Rev., **113**, pp. 1046–1051.
[4] Holland, M. G., 1963, ''Analysis of Lattice Thermal Conductivity,'' Phys. Rev., **132**, pp. 2461–2471.
[5] Tiwari, M. D., and Agrawal, B. K., 1971, ''Analysis of the Lattice Thermal Conductivity of Germanium,'' Phys. Rev. B, **4**, pp. 3527–3532.
[6] Sood, K. C., and Roy, M. K., 1993, ''Longitudinal Phonons and High-Temperature Heat Conduction in Germanium,'' J. Phys.: Condens. Matter, **5**, pp. 301–312.
[7] Asen-Palmer, M., Bartkowski, K., Gmelin, E., Cardona, M., Zhernov, A. P., Inyushkin, A. V., Taldenkov, A., Ozhogin, V. I., Itoh, K. M., and Haller, E. E., 1997, ''Thermal Conductivity of Germanium Crystals With Different Isotopic Compositions,'' Phys. Rev. B, **56**, pp. 9431–9447.
[8] Nilsson, G., and Nelin, G., 1971, ''Phonon Dispersion Relations in Ge at 80 K,'' Phys. Rev. B, **3**, pp. 364–369.
[9] Dove, M. T., 1993, *Introduction to Lattice Dynamics*, Cambridge, Cambridge.
[10] Kittel, C., 1996, *Introduction to Solid State Physics*, Wiley, New York.
[11] Geballe, T. H., and Hull, G. W., 1958, ''Isotopic and Other Types of Thermal Resistance in Germanium,'' Phys. Rev., **110**, pp. 773–775.
[12] Klemens, P. G., 1958, ''Thermal Conductivity and Lattice Vibrational Modes,'' Solid State Phys., **7**, pp. 1–98.
[13] Slack, G. A., 1957, ''Effect of Isotopes on Low-Temperature Thermal Conductivity,'' Phys. Rev., **105**, pp. 829–831.
[14] Ziman, J. M., 2001, *Electrons and Phonons*, Oxford, Oxford.
[15] McGaughey, A. J. H., and Kaviany, M., 2004, ''Quantitative Validation of the Boltzmann Transport Equation Thermal Conductivity Model Under the Single Mode Relaxation Time Approximation,'' Phys. Rev. B, **69**, 094303, pp. 1–12.
[16] Hamilton, R. A., and Parrott, J. E., 1969, ''Variational Calculation of the Thermal Conductivity of Germanium,'' Phys. Rev., **178**, pp. 1284–1292.
[17] Mazumder, S., and Majumdar, A., 2001, ''Monte Carlo Study of Phonon Transport in Solid Thin Films Including Dispersion and Polarization,'' ASME J. Heat Transfer, **123**, pp. 749–759.
[18] Ju, Y. S., and Goodson, K. E., 1999, ''Phonon Scattering in Silicon Films With Thickness of Order 100 nm,'' Appl. Phys. Lett., **74**, pp. 3005–3007.
[19] Slack, G. A., and Glassbrenner, C., 1960, ''Thermal Conductivity of Germanium From 3 K to 1020 K,'' Phys. Rev., **120**, pp. 782–789.
[20] McGaughey, A. J. H., and Kaviany, M., 2004, ''Thermal Conductivity Decomposition and Analysis Using Molecular Dynamics Simulations. Part II. Complex Silica Structures,'' Int. J. Heat Mass Transfer, **47**, pp. 1799–1816.